Low Viscosity Reversed Hexagonal Mesophases Induced by Hydrophilic Additives

Idit Amar-Yuli,[†,||] Ellen Wachtel,[‡] Deborah E. Shalev,[§] Abraham Aserin,[†] and Nissim Garti*[,†]

Casali Institute of Applied Chemistry, The Institute of Chemistry, The Hebrew University of Jerusalem, Jerusalem 91904, Israel, Faculty of Chemistry, The Weizmann Institute of Science, Rehovot 76100, Israel, and Wolfson Centre for Applied Structural Biology, The Hebrew University of Jerusalem, Jerusalem 91904, Israel

Received: December 4, 2007; In Final Form: January 8, 2008

This study reports on the formation of a low viscosity H_{II} mesophase at room temperature upon addition of Transcutol (diethylene glycol mono ethyl ether) or ethanol to the ternary mixture of GMO (glycerol monooleate)/TAG (tricaprylin)/water. The microstructure and bulk properties were characterized in comparison with those of the low viscosity H_{II} mesophase formed in the ternary GMO/TAG/water mixture at elevated temperatures (35−40 °C). We characterized the role of Transcutol or ethanol as inducers of disorder and surfactant mobility. The techniques used were rheology, differential scanning calorimetry (DSC), wide- and small-angle X-ray scattering (WAXS and SAXS, respectively), NMR (self-diffusion and ^{2}H NMR), and Fourier transform infrared (FTIR) spectroscopies. The incorporation of either Transcutol or ethanol induced the formation of less ordered H_{II} mesophases with smaller domain sizes and lattice parameters at room temperature (up to 30 °C), similar to those found for the GMO/TAG/water mixture at more elevated temperatures (35−40 °C). On the basis of our measurements, we suggest that Transcutol or ethanol causes dehydration of the GMO headgroups and enhances the mobility of the GMO chains. As a result, these two small molecules, which compete for water with the GMO polar headgroups, may increase the curvature of the cylindrical micelles and also perhaps reduce their length. This results in the formation of fluid H_{II} structures at room temperature (up to 30 °C). It is possible that these phases are a prelude to the $H_{II}-L_2$ transformation, which takes place above 35 °C.

Introduction

Surfactant molecules self-assemble in water into a large variety of morphologies, including liquid crystalline phases such as lamellar, cubic, and hexagonal phases.[1−8] The high viscosity of the liquid crystalline phases limits their application and, therefore, raises the need for low viscosity dispersions of liquid crystal phases in aqueous media (e.g., cubosome, hexosome, liposome dispersions).[9−11] However, while dilution with water lowers the viscosity, this process also dramatically decreases the solubilization capacity as well as the stability.[9−11] During the past decade, studies of structural changes in liquid crystals, promoted by hydrophilic/hydrophobic guest molecules, have shown that it is possible to manipulate the curvature of liquid crystalline structures, thereby forming mesophases with somewhat nonconventional properties.[12−16] In some cases, the structural differences may assist in lowering the viscosity of the classic liquid crystal phases, which thereby extends the range of their potential applications.[12,16] Lamellar and discrete cubic mesophases have been shown to exhibit relatively lower viscosities (as compared to hexagonal and bicontinuous cubic phases) and have found application in several biophysical studies (lipolytic processes, proteins entrapment)[17,18] as well as in the production of bioelectrodes and biosensor devices.[19−21]

Significant progress has been made in the formation and characterization of the discontinuous micellar cubic and the sponge phases.[12−15,22] In the monoolein/water system, the addition of hydrophilic molecules such as ethanol, or more hydrophobic molecules such as oleic acid and *R*-(+)limonene, led to the formation of a sponge phase (only in the presence of hydrophilic guest molecules) and a micellar cubic phase ($Fd\bar{3}m$).[12,15,16] The latter phase was formed upon addition of isopropyl myristate (IPM) to the octaethyleneglycol dodecyl ether ($C_{12}EO_8$)/water and lecithin/water systems (I_1 and I_2, respectively).[14]

A few intermediate (also termed "defected") lamellar and hexagonal phases were also reported.[16,22−24] The combination of anionic/amphoteric surfactant mixtures (sodium and triethanol amine salt of polyoxyethylene myristyl ether sulfate (PMST)/*N*-carboxyethyl *N*-hydroxyethyl *N*-aminoethyl dodecylamide (IB)), decane, oleic acid, and water allowed the formation of discontinuous cubic and sponge structures and swollen multilamellar vesicle phases (with ∼30−60 wt % water). In the monoolein-based system, the addition of sodium oleate led to its transformation to a slightly bluish, closed bi- and multilayer vesicle preparation with an even larger water content (up to ∼80 wt %). By modifying the ratio of components, especially the water content, Borné et al. were able to decrease the lamellar viscosity without damaging its entropic stabilization (contrary to the well-known dispersion of liposomes).[16] Sato et al. reported on intermediate lamellar and hexagonal (intermediate ribbon, R_1) phases in polyoxyethylene cholesteryl ether/water systems.[22] The H_1-R_1 phase transformation was attributed to increasing packing constraints caused by the bulky sterol moiety in the lipophilic core and seemed to imply a second-order thermody-

* Corresponding author. Tel.: +972-2-658-6574/5. Fax: +972-2-652-0262. E-mail: garti@vms.huji.ac.il.

[†] Casali Institute of Applied Chemistry, The Hebrew University of Jerusalem.

[‡] The Weizmann Institute of Science.

[§] Wolfson Centre for Applied Structural Biology, The Hebrew University of Jerusalem.

[||] Part of a Ph.D. dissertation.

10.1021/jp711421k CCC: $40.75
Published on Web 03/07/2008

namic phase transition (being different from the L_α to R_1 transition).[22] The ribbon aggregates, formed at ~22−28 wt % water, were described as less elongated and more loosely packed than the H_I phase.[22]

Recently, we reported the existence of a less ordered H_{II} phase in GMO/tricaprylin (TAG)/water mixtures, which was characterized by relatively small lattice parameters and effective crystallite sizes. This structure formed at room temperature with water content below 20 wt %.[25] Upon heating the water-poor mixture (12.5 wt % water) above 35 °C it became fluid, yet the hexagonal symmetry was maintained.[26] The fluidity of the H_{II} phase was explained by a significant reduction in domain size. It also seemed reasonable to assume that the cylinder length decreased as well, as a prologue to the $H_{II}-L_2$ transformation.

The successful production of fluid hexagonal phases at room temperature is essential for the field of injectable medications and for improved qualities of spreading and absorption in pastes. To achieve low viscosity reverse hexagonal phases at room temperature, we have now added polyethylene glycols and alcohols such as diethylene glycol mono ethyl ether (Transcutol) and ethanol, respectively, to the ternary GMO/TAG/water mixture. These additives were tested as absorption enhancers and were found to improve the topical and transdermal delivery of various molecules (vitamins and their derivatives, ascorbyl palmitate, and drugs such as cyclosporin A, etc.).[27,28] Alcohols have been found to destroy liquid crystal phases,[12,29,30] and ethanol and PEG are able to induce the formation of discontinuous micellar cubic and sponge phases at the expense of the bicontinuous phases.[12,29−31] To study the effect of these additives, we have used polarized light microscopy, rheometry, DSC, X-ray diffraction, and SD-NMR, ^{2}H NMR, and ATR FTIR spectroscopies. We have concentrated on the mixtures GMO/(TAG+Transcutol)/water and GMO/(TAG+ethanol)/water where GMO/TAG+guest molecule is in the weight ratio of 90/10 with 2.75 wt % guest molecule and 12.5 wt % water. To examine the interplay of the various components and the function of the guest molecules, we expanded our study to a range of temperatures (−10 to 40 °C) and compared the results with our previous findings for the ternary mixture (GMO/TAG/water).[26]

Experimental Section

Materials. Monoolein, GMO, and distilled glycerol monooleate that consists of 97.1 wt % monoglyceride and 2.5 wt % diglyceride (acid value 1.2, iodine value 68.0, melting point 37.5 °C, and free glycerol 0.4%) were purchased from Riken (Tokyo, Japan). Tricaprylin (triacylglycerols, TAG; assay 97−98%) was obtained from Sigma Chemical Co. (St. Louis, MO). Ethanol was obtained from Sigma Chemical Co. (St. Louis, MO). Transcutol HP (99.9%) was a kind gift from Gattefossé (Cedex, France). D_2O (D, 99.9%) was purchased from Cambridge Isotope Laboratories, Inc. (Cambridge, MA). Water was double distilled. All ingredients were used without further purification.

Sample Preparation. Hexagonal liquid crystalline samples were formed by mixing all of the components while heating to ~70 °C in sealed tubes under nitrogen (to avoid oxidation of the GMO) for ca. 15 min and then cooling to room temperature.

Light Microscopy. The samples were inserted between two glass microscope slides and observed with a Nikon light microscope equipped with cross-polarizers and attached to a video camera and monitor. The samples were analyzed between room temperature and 50 °C.

Rheological Measurements. Rheological measurements were performed using the Rheoscope 1 rheometer (Thermo-Haake, Karlsruhe, Germany). A cone-plate sensor was used with a diameter of 35 mm, cone angle of 1°, and a gap of 0.024 mm. The linear viscoelastic range (LVR) of a material was determined before carrying out the oscillatory measurements. The storage and loss moduli were plotted as a function of stress at frequency $\omega = 1$ Hz, at 25 °C (data not shown). The shear moduli were independent of stress up to a critical applied stress and generally were observed to fall off sharply beyond the values of 100−120 Pa. These results indicate that the samples possess linear viscoelastic properties up to about 100−120 Pa. Above these typical values, the microstructure of the H_{II} phases breaks down, which was reflected by the rapid decrease of the moduli. According to the determined LVR, the viscoelasticity measurements were generally performed at 75 Pa.

Frequency-dependent rheological measurements were conducted in the range of 0.01−100 rad/s. The viscoelasticity of the H_{II} phases was characterized in terms of the elastic and the η^*, from which the complex viscosity G'', the loss modulus G', and the longest relaxation time τ_{max} could be evaluated. All of the tests, performed at 25 °C, were measured in triplicate and found to be reproducible. In the present study, the results obtained for all of the H_{II} phases comply with the Maxwell model only at low frequencies, where the plot G'/G'' against ω is a straight line (data not shown).[32] At higher frequencies, the systems deviated from the Maxwell model, which should display a single relaxation time. For quasi Maxwellian systems, the zero-shear viscosity can be estimated from $G''(\omega_m)$, where $G'(\omega_m)$ and $G''(\omega_m)$ cross each other (eq 1).[33]

$$\eta_0 = 2 \cdot G'(\omega_m) \cdot \tau_{max} \quad (1)$$

Small-Angle X-ray Scattering (SAXS). Scattering experiments were performed using Ni-filtered Cu Kα radiation (0.154) from an Elliott rotating anode X-ray generator that operated at a power rating of 1.2 kW. X-radiation was further monochromated and collimated by a single Franks mirror and a series of slits and height limiters, and measured by a linear position-sensitive detector. The samples were held in 1.5 mm quartz X-ray capillaries inserted into a copper block sample holder. The temperature was maintained at $T \pm 0.5$ °C with a recirculating water bath. The camera constants were calibrated using anhydrous cholesterol. Prior to the diffraction measurements, the samples were incubated at subzero temperature for at least 2 h to facilitate full development of the L_c phase. The scattering patterns were desmeared using the Lake procedure implemented in home-written software.[34] To estimate a lower bound for the sizes of ordered domains (L_H), the full width at half-height of the (10) diffraction peak was measured, and this value was inserted into the Scherrer formula.[35]

Wide-Angle X-ray Scattering (WAXS). WAXS patterns from samples held in 1.5 mm quartz capillaries were obtained on Fuji imaging plates, using a Searle camera equipped with Franks optics, affixed to an Elliott GX6 rotating anode generator operating at 1.2 kW and producing copper radiation ($\lambda = 1.54$ Å). The capillaries were inserted into a copper block, the temperature of which was controlled using a Peltier thermoelectric element (Melcor). Exposure times were on the order of 8 h. The imaging plates were scanned with a He−Ne laser (Spectra Physics-Lexel) in conjunction with a homemade reader based on an Optronics densitometer with computer interface. Prior to the diffraction measurements, the samples were incubated at subzero temperature overnight to facilitate full development of the L_c phase.

Differential Scanning Calorimetry (DSC). A Mettler Toledo DSC822 measuring model system was used. The DSC measure-

ments were carried out as follows: 5−15 mg of hexagonal liquid crystalline samples were weighed, using a Mettler M3 microbalance, in standard 40 μL aluminum pans and immediately sealed by a press. The samples were rapidly cooled in liquid nitrogen from 30 to −20 °C, at a rate of 4 °C min^{-1}. The samples remained at this temperature for 120 min and then were heated at 1 °C min^{-1} to 40 °C. An empty pan was used as a reference. The instrument determined the fusion temperatures of the components and the total heat transferred in any of the observed thermal processes. The enthalpy change associated with each thermal transition was obtained by integrating the area of the relevant DSC peak. DSC temperatures reported here were reproducible to ±0.2 °C.

Pulsed-Gradient−Spin−Echo NMR (PGSE-NMR). The field gradient stimulated pulse−spin−echo program was used to measure diffusion. The measurements were performed on samples between −10 and 40 °C on a Bruker DRX-400 spectrometer, with a BGU II gradient amplifier unit and a 5 mm BBI probe equipped with a *z*-gradient coil, providing a *z*-gradient strength (g) of up to 55 G cm^{-1}. Experiments were carried out by varying g and keeping all other timing parameters constant. The measurements were repeated at least three times. According to the parameters of the experiments (the time between the leading edges of the gradient pulses, Δ, was 300 ms), the possible molecular displacement during the experiment, $\langle r^2 \rangle = 2\Delta D$, is on the order of 1 μm or more. The substructures are smaller than this, such that the measured diffusion coefficient represents the aggregate diffusion.[36,37]

^{2}H NMR. Samples for NMR experiments were prepared using 4% D_2O as part of the water component. The NMR experiments were performed on a Bruker DRX 400 MHz spectrometer operating at a proton frequency of 400 MHz and deuterium frequency of 61.42 MHz, using a 5 mm broadband probe. The proton and deuterium spectra were acquired with 8K and 2K points, with spectral widths of 13 and 200 ppm, respectively. The temperature range between −10 and 40 °C was precise to within 0.2 °C, and samples were allowed to equilibrate for 10 min at each temperature. The spectra were acquired using 16 transients, exponential apodization with line broadening of 20 Hz, and zero filling of 8K and 4K, respectively.

The magnitude of the quadrupolar splitting is shown to follow eq 2:[38]

$$\Delta = \left| \sum P_i(\upsilon_{Qi}) S_i \right| \qquad (2)$$

where S_i is the order parameter of bound water describing the orientation of the fraction of ^{2}H present at site i (P_i). υ_Q is the quadrupolar coupling constant (220 kHz).[38,39] The magnitude of the quadrupolar splitting has been shown to be proportional to the order parameter.[38,39]

Attenuated Total Reflectance Fourier Transform Infrared (ATR FTIR). A ReactIR 4000 model manufactured by Mettler-Toledo (Millersville, USA) equipped with a diamond probe (DiComp) was used to record the FT-IR spectra (pure components and GMO/(TAG+Transcutol or ethanol)/water. The spectra were recorded with 128 scans. The probe was purged with dry air. The procedures were conducted in the 0.6 L glass reactor of the Mettler-Toledo LABMAX system (Schwerzenbach, Switzerland), which includes a glass reactor, propeller stirrer, thermostat unit, and controller unit. The thermostat unit controls the reactor and jacket temperature on the basis of feedback from the temperature sensors in the reactor and in the jacket. Temperature can be controlled either by specifying an end point temperature or by keeping a predetermined temperature difference between the reactor and the jacket. The samples were first heated to 60 °C for 30 min and then cooled to −10 °C (0.25−1 °C min^{-1} for relatively low and high temperatures, respectively) for 2 h. In the measurements of FT-IR spectra as a function of temperature, the mixture was heated stepwise with temperature intervals of 5 °C. After the sample was kept at the desired temperature for 0.5−1 h, the spectra were recorded. The absorbance intensities reported here were reproducible to ±0.005.

Results and Discussion

Bulk Properties of the Low-Viscosity Reverse Hexagonal Phases Containing Transcutol or Ethanol. *Rheology.* We investigated the impact of Transcutol or ethanol concentration on the viscosity of the reverse hexagonal mesophase (H_{II}) formed by the mixture GMO/(TAG+additive): 90/10 by weight, with 12.5 wt % water. Frequency-dependent rheological measurements were performed to determine the storage modulus ($G'(\omega)$), loss modulus ($G''(\omega)$), and the complex viscosity η^* upon addition of 0−2.75 wt % of guest molecules (Transcutol or ethanol). It should be noted that upon addition of ≥3 wt % Transcutol or ethanol, the hexagonal phase disappears and is transformed into a random distribution of micelles. Frequency-dependent rheological measurements were performed to characterize the viscoelasticity of the H_{II} phases. The storage moduli $G'(\omega)$ and the loss moduli $G''(\omega)$ were plotted against the frequency of the applied oscillations (ω).[40] The behavior of the H_{II} phase in the absence of the additives is presented in Figure 1a.

At low frequencies, the GMO/TAG/water system was found to be more viscous than elastic ($G'' > G'$). The viscous regime, at low frequencies, is a characteristic property of viscoelastic fluids. With an increase in angular frequency, both G' and G'' increased monotonically, and, finally, at the crossover point, G' dominated G''. Above the crossover point, the elastic properties of the systems dominate ($G' > G''$), indicating that the stored energy in the structure prevails over the energy that was dissipated by the viscous forces. At frequencies close to the crossover point, the H_{II} phases reveal viscoelastic behavior that can be classified as the "transition to the flow region".[41]

Addition of Transcutol or ethanol resulted in a decrease in the complex viscosity η^* of the mesophases (Figure 1b); however, the general trend of the $G'(\omega)$ and $G''(\omega)$ was consistent with hexagonal structure (Figure 1a), as described by Mezzenga et al.[41] This suggests that the hexagonal mesophase was not damaged (up to 2.75 wt % additive). The complex viscosity η^* of the liquid crystals with 0 and 2.75 wt % of each additive, plotted as a function of frequency (Figure 1b), shows a decrease in the complex viscosity with addition of Transcutol or ethanol. This effect is more pronounced upon addition of ethanol. The viscosity at zero shear rate can be calculated (see Experimental Section) from the complex viscosity and was found to be ~10^4 Pa s in the absence of guest molecules, similar to the GMO-based H_{II} phases reported in the literature.[41] The incorporation of the guest molecules lowered the viscosity to 10^3 Pa s (2.75 wt % of Transcutol or ethanol). Because the major rheological properties of the different phases depend primarily on the topology of the water−lipid interface,[42] we can suggest that the presence of the additives led to changes in the GMO−water interface during the transformation into more fluid behavior.[32,42]

The study of variations of the longest relaxation time (τ_{max}) with composition has been shown to be the most reliable rheological method to detect order−disorder transitions in liquid

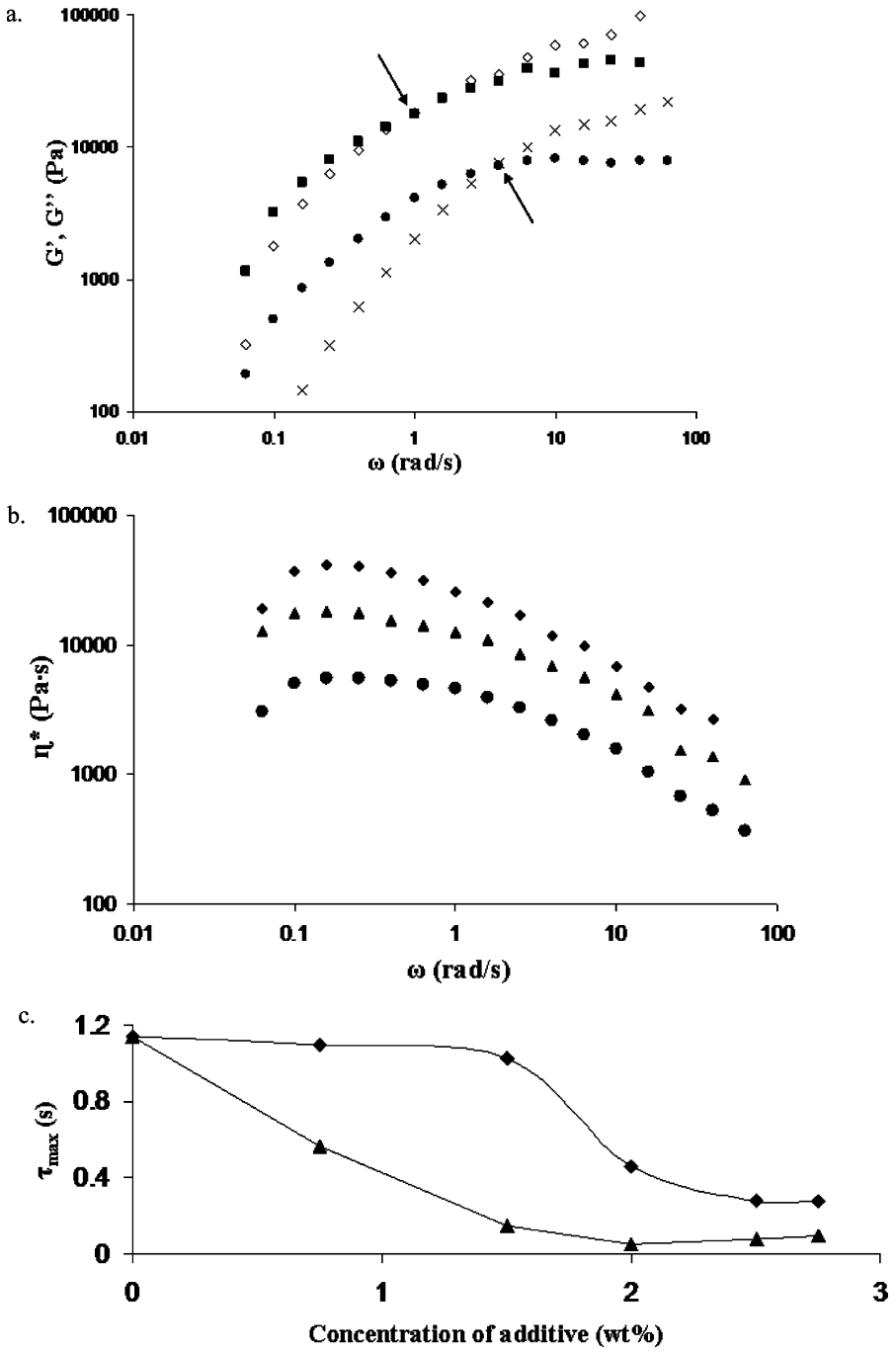

Figure 1. (a) Dynamic frequency sweep test for GMO/TAG/water (G'' (■),G' (◇)) and GMO/(TAG+ethanol)/water (G'' (●),G' (×)) systems containing weight ratio GMO/TAG or GMO/(TAG+additive) 90/10, 12.5 wt % water at 25 °C. The arrow shows the crossover points. (b) Complex viscosity η^* of GMO/tricaprylin/water (◆), GMO/(TAG+Transcutol)/water (▲), and GMO/(TAG+ethanol)/water (●) mesophases, as a function of applied oscillation, all at 25 °C. (c) The longest relaxation time τ_{max} as a function of Transcutol (◆) and ethanol (▲) weight concentrations, all at 25 °C.

crystalline phases.[41,43] τ_{max} can be calculated as the inverse of the frequency at which the crossover takes place ($\tau_{max} = 1/\omega$). In liquid crystals, this parameter is regarded as the time scale for relaxation to the equilibrium configuration of the water−lipid interface, following perturbation by shear deformations.[42] The "liquid-like" behavior, which was obtained upon the addition of Transcutol or ethanol, is reflected in the decrease of τ_{max} with increasing concentrations of the additives (Figure 1c). The addition of Transcutol up to 1.5 wt % (GMO/additive ratio of 52/1 wt/wt) did not change the viscoelastic properties of the H_{II} phase (Figure 1c). However, at 2 wt % (39/1 wt/wt) of added Transcutol, τ_{max} decreased by 67%, and the sample showed plastic behavior consistent with the characteristic of a fluid sample.[42] Above 2 wt % (31−28/1 wt/wt), the viscoelastic properties changed only slightly.

The system into which ethanol was added behaved somewhat differently (Figure 1c). The incorporation of even 0.75 wt % ethanol (104/1 wt/wt) decreased τ_{max} by approximately 50%. Doubling the ethanol concentration (1.5 wt % or 52/1 GMO/ethanol weight ratio) led to an additional decrease in the longest relaxation time (75%), which is attributed to more plastic behavior at the expense of elastic behavior. Further addition of ethanol (>1.5 wt %) only slightly affected the viscoelastic properties of the samples. We therefore concluded that, on a weight basis, ethanol is more efficient in lowering the viscosity and is more effective in inducing the formation of a liquid-like

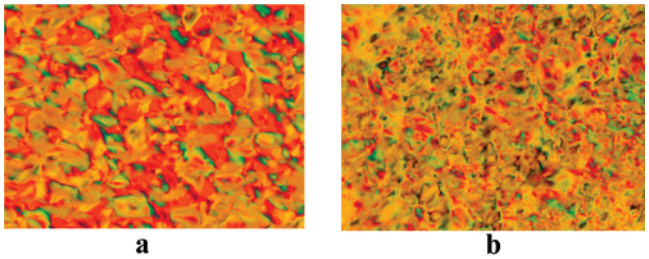

Figure 2. Polarized optical microscope images of fluid H_{II} liquid crystal systems composed of (a) GMO/(TAG+Transcutol)/water and (b) GMO/(TAG+ethanol)/water at room temperature.

(plastic) structure than is Transcutol. Furthermore, larger quantities of ethanol can be used to control the viscoelastic properties of the H_{II} phase without destroying the hexagonal structure. Calculation of the guest molecule content on a molar basis (GMO/additive molar ratio) reveals that at 0.75 wt % of each of the additives, the molar ratio for GMO/ethanol was ~13/1, while that of GMO/Transcutol was 34/1. Only at 2 wt % Transcutol did the molar ratio of GMO/Transcutol reach 14/1. This explains why higher weight levels of ethanol can be used to control the viscoelastic properties of the H_{II} phase without destroying the hexagonal structure.

On the other hand, with 2.75 wt % of each of the additives, the two samples showed somewhat similar liquid-like behavior. In this case, the GMO/Transcutol and GMO/ethanol molar ratios were 11/1 and 4/1, respectively. Hence, on the basis of molar ratio, Transcutol is more effective than ethanol in decreasing the viscosity of the mesophase phase without damaging the H_{II} symmetry. One should bear in mind that the Transcutol molecule is ~3 times longer than ethanol with three hydrogen-bond acceptor sites (one hydroxyl group and two ether bonds), as compared to ethanol, which has only one hydroxyl group. Therefore, equal weights of the additives result in an equal number of hydrogen acceptors sites of both molecules. Ethanol is a hydrotrope by definition, but is incapable of behaving like a surfactant.[44] Hence, on the basis of geometric differences between the two compounds, it is reasonable to assume that the ethanol molecule is incorporated in the vicinity of the surfactant head groups and is more free to rotate than Transcutol. In this way, it may have more effect on the water−GMO interface.

On the basis of these rheological measurements, we decided to focus attention on the GMO/(TAG+Transcutol)/water or GMO/(TAG+ethanol)/water mixtures: GMO/(TAG+guest molecule) at weight ratio of 90/10, with 2.75 wt % guest molecule and 12.5 wt % water. We therefore will characterize the microstructure of the lowest viscosity H_{II} mesophase that formed at room temperature.

Polarized Light Microscopy. Polarized light microscope images of the GMO/TAG/Transcutol/water and GMO/TAG/ethanol/water mixtures at room temperature are shown in Figure 2a,b. Both images displayed birefringent and colorful textures that can be attributed to the hexagonal symmetry, although the samples are fluid (i.e., we can detect sample flow during the measurements).

DSC. Typical DSC thermograms, obtained during heating the GMO/TAG/water, GMO/TAG/Transcutol/water, and GMO/TAG/ethanol/water mixtures, are shown in Figure 3 (thermograms I, II, and III, respectively). The thermotropic behavior of the GMO/TAG/water mixture (Figure 3, thermogram I) during the heating scan from −20 to +40 °C reveals the existence of two rather broad endothermic events with maxima at −1.0 ± 0.2 (peak A) and 6.1 ± 0.2 °C (peak B).[26] There is an additional high temperature shoulder on peak B and a broad plateau that extends from approximately 12 to 26 °C. Identification of the two peaks was discussed previously.[45] Peak A (replacing the water by D_2O resulted in a peak shift of ~1.5 °C)[45] was found to be due to water fusion (with enthalpy of 24 J gr^{-1}). A D_2O shift was not detected for peak B, confirming that the B endotherm is not due to water (i.e., it is not sensitive to the substitution of deuterium for hydrogen). For identification of peak B, GMO, tricaprylin, and different weight ratios of the two components were examined. We concluded that peak B (with enthalpy of 36 J gr^{-1}) is related to the fusion of the "hydrophobic moieties of the GMO" solvated by the TAG.[23]

Upon addition of Transcutol or ethanol, the fusion temperature and enthalpy of the water (ice) decreased significantly, as shown in Figure 3 (thermograms II and III). The water fusion maxima decreased to −5.8 ± 0.2 °C (with enthalpy of 8 J gr^{-1}) and −8.8 ± 0.2 °C (with enthalpy of 4 J gr^{-1}) upon addition of Transcutol or ethanol, respectively. The subzero temperature of peak A (Figure 3, thermogram I) indicates the presence of weakly bound water. The incorporation of "water binding molecules" such as Transcutol or ethanol led to stronger water binding with lower melting temperatures (Figure 3, thermograms II and III).

The incorporation of the guest molecules affected the fusion of the hydrophobic moieties of the GMO molecules (peak B) as well. In the presence of Transcutol or ethanol, the broad endothermic peak was split into two partially overlapping peaks with maxima at 5.2 ± 0.2 and 8.9 ± 0.2 °C (with total enthalpy of 37 J gr^{-1}) and 4.2 ± 0.2 and 8.1 ± 0.2 °C (with total enthalpy of 33 J gr^{-1}), respectively. Additionally, both molecules decreased the fusion temperature of the hydrophobic GMO tails by 1−2 °C. Above 12 °C (the high-temperature boundary of peak B in each thermogram), most of the structure was molten, although this process may not be completed until ~26 °C.

We may conclude that the two guest molecules compete for water with the GMO polar headgroups and lead to dehydration of the surfactant headgroups. The ethanol is more efficient in binding water than the Transcutol. These findings are consistent with the viscoelastic behavior. Additionally, both additives slightly induce the beginning of the fusion process of the hydrophobic moieties (peak onset). It is reasonable to conclude that surfactant dehydration can result in less tightly packed hydrophobic chains, thereby promoting chain melting.

WAXS and SAXS. X-ray scattering was used to identify and confirm the structure of the different phases as well as their compositional boundaries as defined by the endothermic peaks of the DSC thermograms. For both samples (GMO/(TAG+Transcutol)/water or GMO/(TAG+ethanol)/water mixtures), measurements were made during heating from 3 to 40 °C, after overnight incubation at subzero temperature. The X-ray scattering patterns of the GMO/(TAG+Transcutol)/water mixture at approximately 3 °C (2D WAXS) and at 10, 15, 20, 25, 35, and 40 °C (1D SAXS) are shown in Figure 4a−g. The X-ray scattering patterns (WAXS and SAXS) of GMO/(TAG+Transcutol)/water and GMO/(TAG+ethanol)/water mixtures as a function of temperature were similar.

At approximately 3 °C, that is, below the maximum temperature of peak B, the 2D WAXS images of both mixtures (with addition of Transcutol or ethanol) revealed four low angle reflections, which could be indexed as the first four orders of a lamellar phase with interlamellar spacing of 52 Å. The sample with added ethanol displayed significant orientation (data not shown), while the sample with Transcutol was randomly oriented. In addition, there are three wide-angle peaks at 4.74,

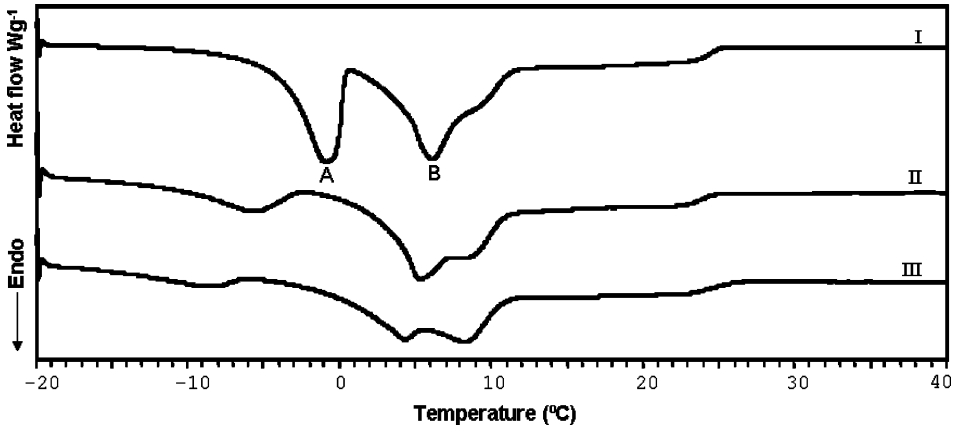

Figure 3. DSC thermograms of (I) GMO/tricaprylin/water mixture with two endothermic events at −1.0 ± 0.2°C (peak A) and 6.1 ± 0.2°C (peak B), (II) GMO/(tricaprylin+Transcutol)/water mixture, and (III) GMO/(tricaprylin+ethanol)/water mixture.

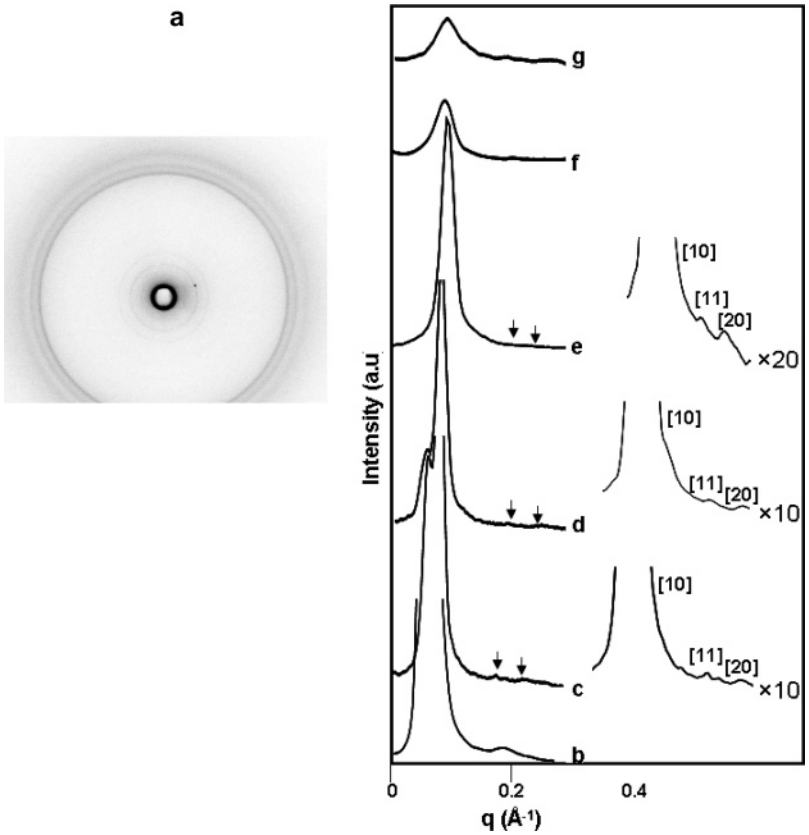

Figure 4. X-ray diffraction patterns of the GMO/(tricaprylin+Transcutol) 90/10 mixture with 12.5 wt % water after overnight incubation at −20 °C, measured at (a) 3 °C (2-D WAXS) and (b) 10, (c) 15, (d) 20, (e) 25, (f) 35, and (g) 40 °C (1-D SAXS). The arrows on traces c, d, and e indicate the locations of the [11] and [20] diffraction peaks.

4.49, and 4.14 Å. The latter are characteristic of a crystalline low-temperature phase, L_c.[3] Such a phase has been previously identified for GMO/water and GMO/TAG/water mixtures following extended low temperature incubation.[3,26] At 10 °C (Figure 4b), the SAXS profile of GMO/(TAG+Transcutol)/water shows two broad Bragg peaks, which can be associated with the lamellar phase, with interlamellar spacing of 52 Å and domain size (based on the width of the first peak) of 300 ± 50 Å. At 15−20 °C (Figure 4c,d), the SAXS profiles give evidence of the existence of a biphasic region. The first peak of a lamellar phase is present in addition to the (10), (11), and (20) reflections of a 2D hexagonal liquid crystalline phase.

At temperatures above 20 °C (25 °C in Figure 4e), three peaks are observed, which can be indexed as the (10), (11), and (20) reflections of a 2D H_{II} phase. Such a structure is visualized as consisting of cylindrical surfactant micelles arranged on a 2D hexagonal lattice.[46] In this temperature range, the intensity of the higher order peaks decreases with increase in temperature, without an increase in the main peak intensity. This phenomenon was observed earlier by Ivanova et al. in a system composed of Pluronic P105 ($(EO)_{37}(PO)_{58}(EO)_{37}$)/water upon addition of polyols.[30] The decrease in intensity of the higher order peaks was associated with the changing electron density of the compounds upon addition of the glycol (changing the contrast between the solvent and the surfactant). They also claimed possible rearrangements in the microstructure upon glycol incorporation. Upon increasing the temperature from 15 to 30 °C, the lattice parameter of the H_{II} structure decreased (Table 1). This effect can be explained either by a dehydration of the surfactant polar headgroups or by an increase in the hydrocarbon

TABLE 1: Lattice Parameters and Effective Crystallite Sizes (a and L_H, Respectively) of the Hexagonal Structures in GMO/TAG/Transcutol/Water Mixture (12.5 wt % Water Concentration) as a Function of Temperature

temperature (°C) ±0.5 °C	a (Å) ±0.5 Å	L_H (Å) ±50 Å
15.0	49.8	446
20.1	49.9	411
25.0	45.8	430
30.2	44.8	286
35.4	N.A.	217
40.1	N.A.	180

chain mobility.[3,47] In addition, there was a decrease in the effective crystallite size (430−180 Å), which was most pronounced between 25 and 40 °C. Previously we showed that addition of a hydrophilic polymer, which competed for water with the GMO polar headgroups, or elevated temperatures (35−40 °C), led to a dehydration process.[25,26] This led to a reduction in L_H and in the lattice parameter values. Furthermore, in the GMO/TAG/water mixture with increasing temperature up to 45 °C, the H_{II} phase was progressively disordered until it was completely disrupted. During this process, a fluid H_{II} phase was formed between 35 and 40 °C with relatively small effective crystallite size (385 Å at 40 °C) and lattice parameter (44.3 Å).[26] Between 35 and 40 °C (Figure 4f,g), only a single broad peak can be observed, implying random distribution of micelles. From the three peak positions and the (10) peak line breadth, we calculated the corresponding mean lattice parameter (a) and the effective crystallite size (L_H) of the hexagonal structures. When only a single broad peak was observed (such as in Figure 4e,g), the effective domain size was calculated from the single peak, for comparison with the H_{II} phases. The results are summarized in Table 1.

We conclude that the incorporation of either Transcutol or ethanol induced the formation of the less-ordered H_{II} structures with smaller domain size and lattice parameters at room temperature (up to 30 °C), similar to the GMO/TAG/water at more elevated temperatures (35−40 °C). The formation of a reverse hexagonal phase with somewhat nonconventional properties is consistent with the work of Sato et al., who reported on a hexagonal to intermediate hexagonal (ribbon, R_1) phase transformation.[22] This second-order phase transition led to a less elongated and more loosely packed structure than the H_I phase.[22]

On the basis of the rheological behavior, polarized light microscopy, SAXS/WAXS, and DSC, we suggest that addition of either Transcutol or ethanol has structural effects similar to those of increasing temperature in that it causes an increase in the mobility of both the water and the GMO chains.[3,25,26] These two small molecules, which compete for water with the GMO polar headgroups, may increase the curvature and partially dehydrate the headgroups. As a result, less-ordered, fluid H_{II} structures with small domains are formed at room temperature (up to 30 °C). It is possible that these phases are a prelude to the $H_{II}-L_2$ transformation, which takes place above 35 °C (Figure 4e,f, Table 1).

Temperature Dependence of the Microstructure of Fluid H_{II} Phases Containing Transcutol or Ethanol. We used PGSE-NMR, ^{2}H NMR, and FTIR spectroscopy to characterize the microstructure of the fluid H_{II} phases composed of GMO/(TAG+Transcutol)/water and GMO/(TAG+ethanol)/water (GMO/TAG+2.75 wt % guest molecule in the weight ratio of 90/10, 2.75 wt % guest molecule and 12.5 wt % water) as a function of temperature.

PGSE-NMR. The self-diffusion coefficients of water (D_W), TAG (D_{TAG}), Transcutol (D_T), ethanol (D_E), and GMO (D_{GMO}) measured using the ^{1}H NMR PGSE technique between −10 and 40 °C for both mixtures are shown in Figure 5$a_{1,2}$−$b_{1,2}$. The diffusion coefficients characterize the mobility of the five components of the mesophase in three temperature regions: −10 to 10, 10−30, and 30−40 °C.

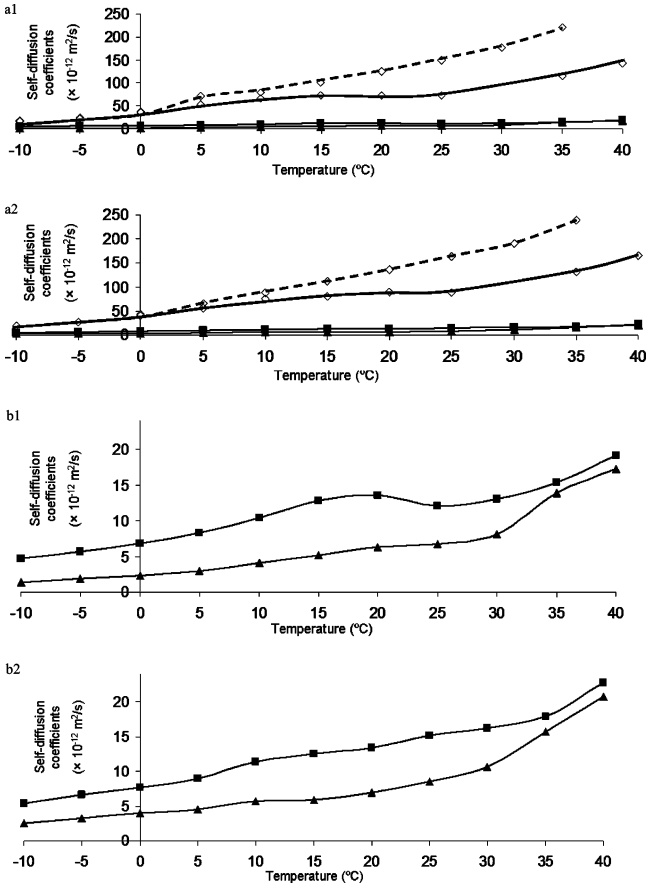

Figure 5. Self-diffusion coefficients of (a) water (◇, dashed line), TAG (■), and GMO (▲), (a_1) (◇, solid line) for Transcutol and (a_2) (◇, solid line) for ethanol, from −10 to 40 °C, and ($b_{1,2}$) GMO (▲) and TAG (■) from −10 to 40 °C, measured by the ^{1}H NMR PFGSE technique for GMO/(TAG+Transcutol)/water and GMO/(TAG+ethanol)/water (12.5 wt % water) mixtures in a_1,b_1 and a_2,b_2, respectively.

−10 to 10 °C. In this temperature range, D_W, D_T, and D_E are of the order of magnitude of 10^{-11} m^2 s^{-1} (Figure 5a_1,a_2) in contrast to D_{GMO} and D_{TAG}, which are of the order of magnitude of 10^{-12} m^2/s (Figure 5$b_{1,2}$). Comparison between the mixture containing Transcutol (Figure 5a_1,b_1) and that containing ethanol (Figure 5a_2,b_2) reveals that all of the self-diffusion coefficients are similar in each of the mixtures. Up to 10 °C, the water, transcutol, and ethanol diffusion coefficients increase gradually (10^{-11} m^2 s^{-1}). We may assume that incubation at −10 °C is not sufficient to crystallize the water because both additives impart a very large supersaturation effect. This assumption is in agreement with the fact that the melting of the water (ice) at −5.8 ± 0.2 and −8.8 ± 0.2 °C for the samples that contained Transcutol and ethanol, respectively, is only observed when the samples are incubated at −20 °C (Figure 3) and not at −10 °C (data not shown). The diffusion coefficients of the TAG molecules are only slightly larger than those of GMO (by 3−6 × 10^{-12} m^2/s Figure 5b_1,b_2) as compared to 1 order of magnitude difference between GMO and TAG in the absence of the guest molecules. Hence, we suspect that the presence of the guest molecules affects the miscibility of TAG in GMO and this can lead to deeper incorporation of TAG between the tails of the GMO.[26] The effect on the miscibility of TAG in

GMO is in agreement with the changes that were observed in the fusion peak of the surfactant tails for the samples that contained Transcutol and ethanol (Figure 3).

10−30 °C. Further heating of the mixture led to an increase in the diffusion coefficients of all of the components (Figure 5). At 10 °C, where the L_C structure exists in both mixtures, D_W is 80 × 10^{-12} m^2 s^{-1} and D_T and D_E are 70 × 10^{-12} m^2 s^{-1}. Upon further increasing the temperature, the H_{II} phase is dominant, but a small amount of L_C structure remains. The free water diffusion coefficients increase more strongly in the cylinder cores than those of the Transcutol and ethanol. Up to 25 °C, D_T and D_E almost do not change (80 × 10^{-12} m^2 s^{-1}), while D_W increases by a factor of 2 (155 × 10^{-12} m^2 s^{-1}). These results may imply that at this temperature range the additives are strongly interacting at the interface and hence are not able to move freely within the cylinder core as does the water.

Beginning at 10 °C, the diffusion coefficient of both TAG and GMO, which is the least mobile in each mixture, increases. The increase in the mobility of TAG and GMO can be associated with the transition of the hydrocarbon chains from a rigid conformation to one that is liquid-like. The explanation for these results is in agreement with the completion of the 8.9 °C DSC peak, which was attributed to the melting of hydrophobic moieties (Figure 3). They are also supported by X-ray measurement that showed the presence of L_C phase prior to the hydrophobic transition.

As shown by the X-ray data (Figure 4), cylinders are the dominant aggregate form above 10 °C at the expense of the lamellar crystalline structure. At 25 °C only H_{II} is present; however, its structure becomes less ordered. When comparing the diffusion coefficients of the components upon addition of Transcutol and ethanol at room temperature to those measured in their absence at elevated temperatures (35−40 °C), we see: (1) The diffusion coefficient of water is much higher in the presence of the guest molecules (155 × 10^{-12} m^2 s^{-1} instead of 60 × 10^{-12} m^2 s^{-1}).[26] The presence of hydrophilic additives can modify the equilibrium of water molecules hydrating the polar headgroups of the surfactant, by introducing stronger hydrogen-bond acceptors.[48] Therefore, highly hydrophilic polyols and ethanol can act as "water pumps", as we have observed, and have an effect analogous to that of electrolytes in phospholipid-based liquid crystals.[48] (2) In GMO/TAG/water, at 35−40 °C, the TAG and GMO diffusion coefficients were 10 and 15 × 10^{-12} m^2 s^{-1}, respectively.[26] Similarly, at 25 °C in the presence of Transcutol or ethanol, the corresponding coefficients are 10 and 15 × 10^{-12} m^2 s^{-1}. Therefore, the major effect of the addition of Transcutol or ethanol on the self-diffusion of the components of the ternary mixture is to increase the mobility of the water. This result implies that in this temperature range the additives are strongly interacting at the interface and in the inner cylinders.

^2H NMR. We measured the ^2H NMR quadrupolar splitting over the temperature range from −10 to 40 °C for the 90/10 mixtures of GMO/(TAG+transcutol) or GMO/(TAG+ethanol) with 12.5 wt % water (of which 4% was deuterium oxide). The magnitude of the quadrupolar splitting has been shown to be proportional to the order parameter (see the Experimental Section).[39] The quadrupolar splitting of the GMO/(TAG+transcutol)/D_2O−H_2O system, at 25, 35, and 40 °C, is shown in Figure 6a−c. Similar results were obtained for the two systems. At 25 °C, a single quadrupolar splitting can be detected at ∼900 Hz, with an additional isotropic peak, which implies an anisotropic environment for the deuterium (Figure 6a). We can conclude that the cylinders of the H_{II} phase are aligned with respect to the magnetic field of the spectrometer.[49−51] It is possible that the increased fluidity of the H_{II} phase facilitates alignment even at this relatively low temperature as compared to the necessity of thermal treatment in the absence of Transcutol or ethanol.[26] Additionally, the incorporation of each additive decreased the magnitude of the quadrupolar splitting as compared to the ternary mixture (∼1000 and ∼2000 Hz). Because the splitting magnitude has been shown to be proportional to the order parameter, it could suggest that this technique shows that the fluid H_{II} mesophases possess less ordered structures.[39,49−51] Upon further heating of the mixture to 35 °C, an isotropic peak with higher intensity appeared in addition to the very low-intensity split pair (Figure 6b). At 40 °C, only a single sharp isotropic peak can be seen in Figure 6c. This result is consistent with the formation of the L_2 phase, which was revealed by SAXS.

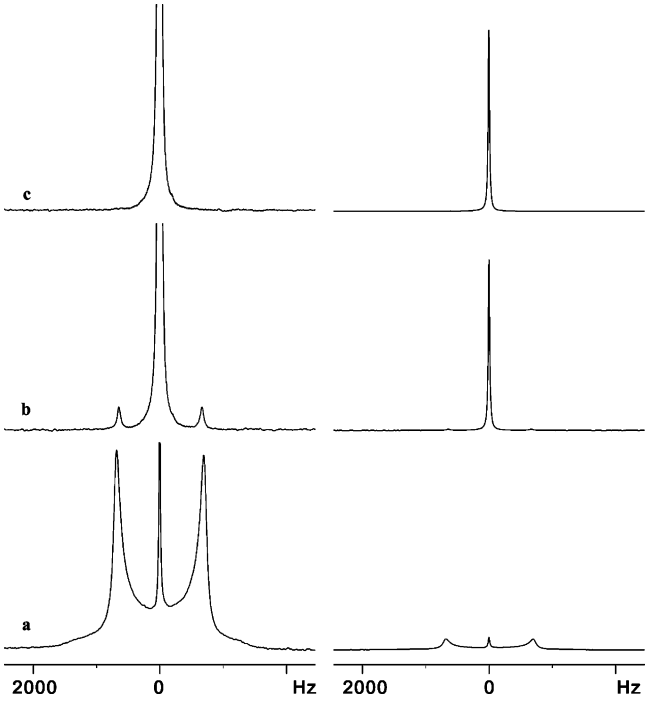

Figure 6. ^2H NMR (1D) spectra of GMO/(TAG+Transcutol)/12.5 wt % water at (a) 25, (b) 35, and (c) 40 °C. Left panel shows ∼20× magnified spectra.

ATR-FTIR. The molecular structure of GMO and the FTIR spectrum for the GMO/(TAG+trancutol)/12.5 wt % water mixture at 25 °C are shown in Figure 7. We focused on four major bands indicated in the figure to analyze the conformation of the surfactant molecule and its interaction with water in the different mesophases as a function of temperature (−10 to 40 °C).

We analyzed the structure in terms of three regions: the water-rich core, the water−surfactant interface, and the lipophilic acyl chain region. The absorption bands at 3200−3400 cm^{-1}, which are attributed to the O−H stretching modes (ν_{OH}), are used to characterize the interactions of the O−H groups (at the β and γ positions on the GMO headgroups) of the surfactant and water molecules. The stronger is the hydrogen bonding between the surfactant and the water, the lower is the stretching frequency of the O−H group (ν_{OH}). At the interface, two major vibrational modes can be observed, which reflect the interfacial arrangement of the lipid headgroups. For GMO, these include the stretching of the bonds CO−O (ester at the α position, ∼1180 cm^{-1}) and C═O (carbonyl at the α position, 1720−1740 cm^{-1}).[52,53] The carbonyl band consists of two components,

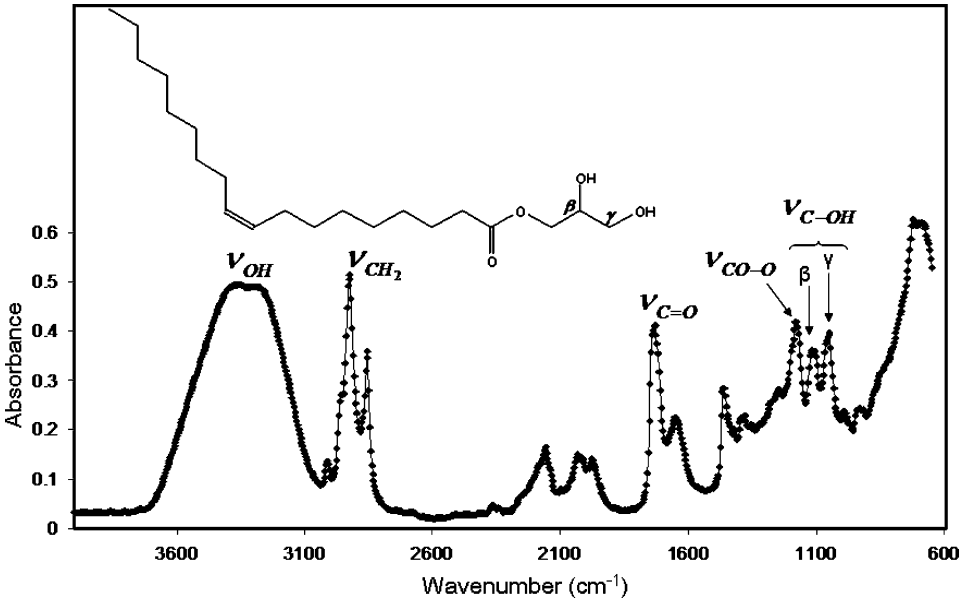

Figure 7. Molecular structure of GMO and the FTIR spectrum obtained for a GMO/(TAG+Transcutol)/water mixture with 12.5 wt % water at 25 °C. The symbols marked on several absorption bands are explained in the text.

one originating from "free" (freely rotating) carbonyl (1740 cm^{-1}) and the second from intramolecular hydrogen-bonded carbonyl groups (1730 cm^{-1}).[52] Information about the conformational order of the acyl chains is obtained from the stretching modes of the CH_2 segments (ν_{CH_2}). The stretching modes of the GMO methylene groups are observed at ~2853 cm^{-1} (symmetric stretching) and at ~2918 cm^{-1} (antisymmetric stretching).[52]

Water-Rich Core. The temperature dependence of the infrared spectra of the GMO/(TAG+Transcutol)/water and GMO/(TAG+ethanol)/water mixtures in the range of 3000−3700 cm^{-1} can be seen in Figure 8a$_{1,2}$, respectively. In the mixture containing Transcutol, at −10 °C a major stretching absorption band (ν_{OH}) was detected at 3265 cm^{-1} with an additional shoulder at 3377 cm^{-1} (γ and β positions of GMO, respectively, Figure 8a$_1$). In the presence of ethanol (instead of Transcutol) at −10 °C, the high-intensity major band (ν_{OH}) was detected at 3261 cm^{-1} with an additional shoulder at 3362 cm^{-1} (Figure 8a$_2$). This should be compared to the FTIR results in the absence of these guest molecules that showed two poorly resolved maxima at 3238 and 3296 cm^{-1}.[26] We can see that in the presence of both molecules the ν_{OH} values are higher than in their absence. Furthermore, the stretching frequencies of the O−H groups upon addition of Transcutol are higher than in the presence of ethanol. We can conclude that in the presence of each additive, at this temperature, there is less hydrogen bonding between the hydrophilic GMO head groups and water. However, in the mixture containing ethanol, more hydrogen bonds can be detected than in the mixture containing Transcutol.

When the temperature is raised to −5 °C, in the presence of Transcutol or ethanol, the ν_{OH} values increased by 12 cm^{-1} for the γ position and by 7 cm^{-1} for the β position. It should be noted that in the absence of these guest molecules, at this temperature the ν_{OH} increased by 60 and 70 cm^{-1} for the γ and β positions, respectively.[26] In addition, two poorly resolved maxima were detected in the absence of the guest molecules as compared to a major band with an additional shoulder (Figure 8a$_{1,2}$) upon their incorporation. The higher frequencies of both OH groups upon addition of the hydrogen-bonded molecules can imply less hydrogen bonding between the hydrophilic GMO head groups and the water at these temperatures.[54] We may conclude that in this temperature range, the hydrogen bonds are mostly between the water and the guest molecules. Hence, we do not detect frozen water, and only a small increase in the ν_{OH} positions can be seen. These results are in agreement with the DSC measurements that revealed that incubation at −10 °C in the presence of one of the additives led to the disappearance of the water (ice) fusion peak.

Between −5 and 10 °C, in both systems, the absorption intensity of the O−H band at the β position increased at the expense of that of the O−H absorption at the γ position. This indicates that a fraction of the hydrogen bonds between O−H groups (γ position) and water/guest molecules are broken at this temperature (−5 to 0 °C). Additionally, at 10 °C in the presence of ethanol, the ν_{OH} values (β position) decreased by 11 cm^{-1}. This reduction in frequency is also observed in the GMO/TAG/water mixture (at 15 °C) and may be explained through the restriction of the headgroup surface area due to dehydration of the headgroups and increasing curvature and H_{II} formation.[52]

Increasing the temperature to 25 °C, where both samples are fluid yet the hexagonal symmetry is maintained, the two O−H absorption bands gradually decrease in peak height and also broaden, similar to the behavior of the GMO/TAG/water mixture at higher temperatures.[26] This result implies the existence of a less ordered structure (in the water-rich core area) for both fluid systems.[48,52,53]

Water−Surfactant Interface. In both systems, the $C_\alpha O-O$ stretching mode (~1180 cm^{-1}) was relatively insensitive to the lamellar−fluid hexagonal transition (data not shown). Up to 20 °C, the maximum ester group stretching absorption was detected at 1181 cm^{-1}, while the peak height decreased and the line-width increased with increasing temperature. Above this temperature, the frequency decreased to 1176 cm^{-1}. In the GMO/TAG/water mixture, the same tendency was observed at the L_C-H_{II} and H_{II}−fluid H_{II} transitions.[26] It has been proposed[52,55] that a low-frequency shift of the CO−O band may be interpreted as a slight deviation from the dihedral angle of 180° in the $C_\gamma-C_\beta-C_\alpha O-O-C$ segment, induced by torsional motions or by a small population of gauche conformers near the CO−O bond.[52,55] It should be pointed out that for pure GMO

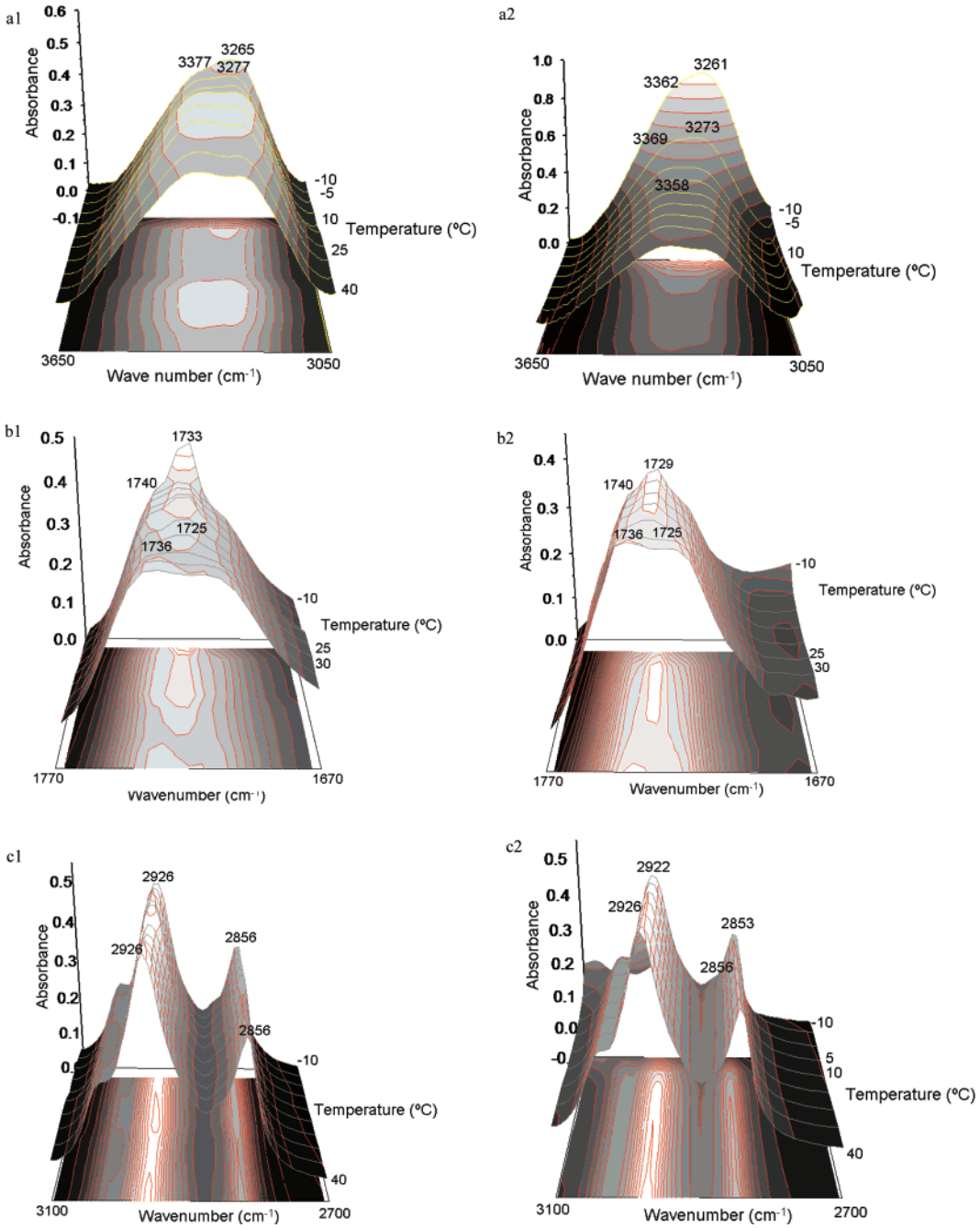

Figure 8. FTIR spectra obtained for GMO/(TAG+Transcutol)/water and GMO/(TAG+ethanol)/water mixtures at various temperatures between −10 and 40 °C in the frequency ranges: ($a_{1,2}$) 3000−3600, ($b_{1,2}$) 1670−1770, and ($c_{1,2}$) 2700−3100 cm^{-1}. Temperatures in °C are indicated in the figure. Parts a_1,b_1,c_1 and a_2,b_2,c_2 relate to the mixtures containing Transcutol and ethanol, respectively.

and TAG at room temperature, the CO−O band is found at 1180 and 1156 cm^{-1}, respectively. Following this interpretation, and according to the pure GMO, TAG, and GMO/TAG/water mixture data, we can conclude that TAG, temperature, Transcutol, and ethanol have a similar effect on the dihedral angle in GMO. This is consistent with the fact that they increase the curvature and lead to a more restricted interface with the formation of H_{II} and fluid H_{II} phases as compared to the lamellar crystalline phase and compared to the L_α phase at room temperature.[55]

The changes in the carbonyl bands as a function of temperature are shown in Figure 8$b_{1,2}$. In the GMO/(TAG+Transcutol)/water and GMO/(TAG+ethanol)/water mixtures, up to 25 °C, the major carbonyl band ($\nu_{C=O}$) was detected at 1733 and 1729 cm^{-1}, respectively, with an additional shoulder at 1740 cm^{-1} (free carbonyl band). Upon increasing the temperature from −10 to 20 °C, the intensity of the free carbonyl increased at the expense of the hydrogen-bonded carbonyl (lower $\nu_{C=O}$). Raising the temperature above 20 °C, in both mixtures, caused the lower frequency C═O band to transform into a shoulder, with a shift to 1725 cm^{-1}. Hydrogen bonding is known to be responsible for the shift to lower frequency.[52] Simultaneously, the intensity of the free carbonyl stretching band increased and remained at 1740 cm^{-1}. Furthermore, at 30 °C the less hydrated carbonyl vibrations band (1740 cm^{-1}) shifted to lower frequencies (by 4 cm^{-1}). It is known that dehydration takes place once the H_{II} phase is formed and as the temperature increases, and in both cases the headgroup surface area decreases.[48] These results suggest that the GMO is dehydrated with increasing temperature (as was seen in the ternary mixture) and the interface is more

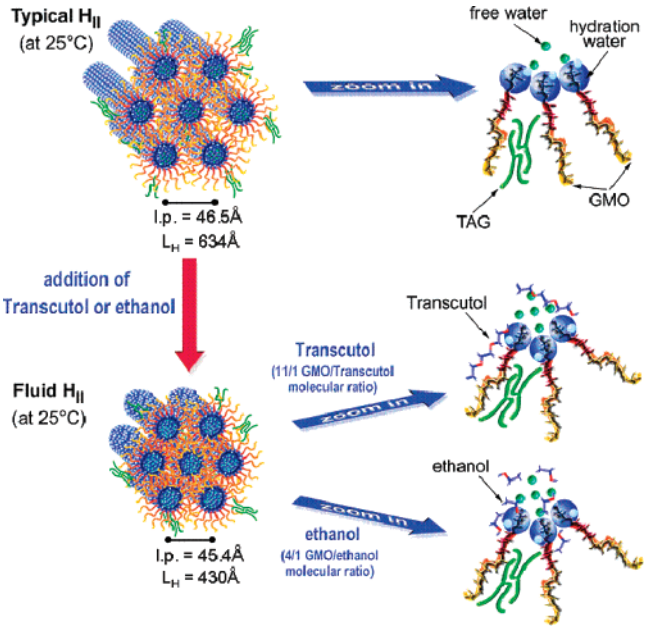

Figure 9. A cartoon illustrating the room-temperature structural and physicochemical properties of the fluid mesophases containing Transcutol and ethanol as compared to those in their absence. l.p. and L_H correspond to the mean lattice parameter and the effective crystallite size in the hexagonal mesophase. It should be noted that the molecular ratio between all of the components should not be concluded from the image. The calculated ratios are GMO/TAG 14/1 in the ternary system and 12/1 in the quaternary.

tightly packed, probably due to a further increase in the curvature (even compared to the situation in the absence of the additives).

Hydrocarbon Chain Region. Between −10 and 40 °C, in the GMO/(TAG+transcutol)/water mixture, the methylene stretching ν_{CH_2} of the hydrocarbon chains of GMO was observed (Figure 8c$_1$) at ∼2856 cm^{-1} (symmetric stretching) and at ∼2926 cm^{-1} (asymmetric stretching). In the alcohol-containing mixture at −10 °C, the methylene stretching vibrations (ν_{CH_2}) were observed (Figure 8c$_2$) at ∼2853 cm^{-1} (symmetric stretching) and at ∼2922 cm^{-1} (asymmetric stretching). Following the behavior of the symmetric stretching mode (in the presence of ethanol) with temperature reveals an upward shift (3 cm^{-1}) at 5 °C, while the asymmetric stretching mode shifted to higher frequencies (4 cm^{-1}) only at 10 °C. In both mixtures, the CH_3 stretching mode, which is observed at 2953 cm^{-1} up to 20 °C, shifts to a 4 cm^{-1} higher frequency at 25 °C. It is known[54,56] that ν_{CH_2} is sensitive to the conformation of the hydrocarbon chain and it shifts upward with an increase in the fraction of gauche conformers. The latter results in increased chain disorder and looser acyl chain packing.[56] Thus, in the mixture containing ethanol, we can identify the chain melting in the range of 5−10 °C. As was previously reported,[26] a similar tendency was observed in the absence of these guest molecules; however, the ν_{CH_2} values were lower by 3−8 cm^{-1} and only above 25 °C reached 2856 and 2925 cm^{-1} (symmetric and asymmetric stretching, respectively). We can conclude that the incorporation of the Transcutol and ethanol increased chain disorder and led to looser acyl chain packing even at very low temperatures, which probably contributes to the formation of the fluid H_{II} structure at low temperature. However, contrary to the hydrophilic part of the surfactant molecule, the effects of Transcutol in the hydrophobic region were more pronounced even at lower temperatures (subzero).

Conclusions

The addition of two polar solvents (dermal penetration enhancers), Transcutol and ethanol, to ternary mixtures of GMO/TAG/water has been investigated to improve our understanding of low viscosity H_{II} phases at room temperature. The microstructural characterization of the quaternary system has been accomplished by optical microscopy, rheology, WAXS, SAXS, and DSC. NMR (self-diffusion and ^{2}H NMR) and FTIR spectroscopies were used to evaluate conformational modifications at the molecular level. We show that addition of Transcutol or ethanol to the GMO/TAG/water mixture leads to the formation of a room-temperature fluid H_{II} phase that has very valuable physical characteristics and properties. Controlling the viscoelastic properties of surfactant-based liquid crystals is a key determinant in controlling the kinetics of release of active molecules through the hydrophilic/hydrophobic interface.

We focused on the GMO/(TAG+Transcutol or ethanol)/12.5 wt % water mixtures with 2.75 wt % guest molecules that formed the lowest viscosity H_{II} structures at room temperature. A schematic representation of the modifications taking place in the H_{II} microstructure upon addition of each additive is presented in Figure 9. This figure is drawn based on the structural understanding that was derived from the results of all of the experimental techniques. The typical H_{II} phase is formed in the absence of additives and exhibits free flow of water in the core of the cylindrical GMO micelles. The micelles pack in a two-dimensional hexagonal lattice (Figure 9, upper part). Upon addition of Transcutol or ethanol, the hexagonal phase is liquefied with reduced domain size, yet with its symmetry retained. The presence of the strong hydrogen-bonding acceptors (hydrophilic guest molecules) in the water core of the cylinders and at the interface decreased the number of water molecules available to hydrate the GMO headgroups (Figure 9, lower part). This effect was more prominent in the presence of ethanol than of Transcutol. The dehydration process enhanced the mobility of the hydrocarbon chains, resulting in increased curvature and concomitant reduction of the lattice parameter.

References and Notes

(1) Larsson, K. *J. Phys. Chem.* **1989**, *93*, 7304−7314.
(2) Misquitta, Y.; Caffrey, M. *Biophys. J.* **2001**, *81*, 1047−1058.
(3) Caffrey, M. *Biochemistry* **1987**, *26*, 6349−6363.
(4) Frank, C.; Sottmann, T.; Stubenrauch, C.; Allgaier, J.; Strey, R. *Langmuir* **2005**, *21*, 9058−9067.
(5) Pena dos Santos, E.; Tokumoto, M. S.; Surendran, G.; Remita, H.; Bourgaux, C.; Dieudonne, P.; Prouzet, E.; Ramos, L. *Langmuir* **2005**, *21*, 4362−4369.
(6) Mezzenga, R.; Schurtenberger, P.; Burbidge, Á.; Michel, M. *Nature Materials* **2005**, *4*, 729−740.
(7) Shearman, G. C.; Khoo, B. J.; Motherwell, M. L.; Brakke, K. A.; Ces, O.; Conn, C. E.; Seddon, J. M.; Templer, R. H. *Langmuir* **2007**, *23*, 7279−7285.
(8) Zeng, X. B.; Liu, Y. S.; Imperor-Clerc, M. *J. Phys. Chem. B* **2007**, *111*, 5174−5179.
(9) Yaghmur, A.; de Campo, L.; Sagalowicz, L.; Leser, M. E.; Glatter, O. *Langmuir* **2006**, *22*, 9919−9927.
(10) Dong, Y. D.; Larson, I.; Hanley, T.; Boyd, B. J. *Langmuir* **2006**, *22*, 9512−9518.
(11) Almgren, M.; Borné, J.; Feitosa, E.; Khan, A; Lindman, B. *Langmuir* **2007**, *23*, 2768−2777.
(12) Efrat, R.; Aserin, A.; Kesselman, E.; Danino, D.; Wachtel, E. J.; Garti, N. *Colloids Surf., A* **2005**, *299*, 133−145.
(13) Engstrom, S.; Wadsten-Hindrichsen, P.; Hernius, B. *Langmuir* **2007**, *23*, 10020−10025.
(14) Kunieda, H.; Horii, M.; Koyama, M.; Sakamoto, K. *J. Colloid Interface Sci.* **2004**, *236*, 78−84.
(15) Pouzot, M.; Mezzenga, R.; Leser, M.; Sagalowicz, L.; Guillot, S.; Glatter, O. *Langmuir* **2007**, *23*, 9618−9628.
(16) Borné, J.; Nylander, T.; Khan, A. *Langmuir* **2001**, *17*, 7742−7751.

(17) Razumas, V.; Larsson, K.; Miezis, Y.; Nylander, T. *J. Phys. Chem.* **1996**, *100*, 11766−11774.
(18) Caboi, F.; Nylander, T.; Razumas, V.; Talaikytë, Z.; Monduzzi, M.; Larsson, K. *Langmuir* **1997**, *13*, 5476−5483.
(19) Rowinski, P.; Bilewicz, R.; Stebe, M.-J.; Rogalska, E. *Anal. Chem.* **2002**, *74*, 1554−1559.
(20) Barauskas, J.; Razumas, V.; Talaikytë, Z.; Bulovas, A.; Nylander, T.; Tauraitë, D.; Butkus, E. *Chem. Phys. Lipids* **2003**, *123*, 87−97.
(21) Rowinski, P.; Bilewicz, R.; Stebe, M.-J.; Rogalska, E. *Anal. Chem.* **2004**, *76*, 283−291.
(22) Sato, T.; Hossain, K.; Acharya, D. P.; Glatter, O.; Chiba, A.; Kunieda, H. *J. Phys. Chem. B* **2004**, *108*, 12927−12939.
(23) Watanabe, K.; Nakama, Y.; Yanaki, T.; Thunig, C.; Horbachek, K.; Hoffmann, H. *Langmuir* **2004**, *20*, 2607−2613.
(24) Constantin, D.; Oswald, P.; Impéror-Clerc, M.; Davidson, P.; Sotta, P. *J. Phys. Chem. B* **2001**, *105*, 668−673.
(25) Amar-Yuli, I.; Wachtel, E.; Ben-Shoshan, E.; Danino, D.; Aserin, A.; Garti, N. *Langmuir* **2007**, *23*, 3637−3645.
(26) Amar-Yuli, I.; Wachtel, E.; Shalev, D. E.; Moshe, H.; Aserin, A.; Garti, N. *J. Phys. Chem. B* **2007**, *111*, 13544−13553.
(27) Femenia-Font, A.; Padula, C.; Marra, F.; Balacuer-Fernandez, C.; Merino, V.; Lopez-Castellano, A.; Nicoli, S.; Santi, P. *J. Pharm. Sci.* **2006**, *311*, 182−186.
(28) Liu, H. Z.; Li, S. M.; Wang, Y. J.; Tao, H. M.; Zhang, Y. *Int. J. Pharm.* **2006**, *95*, 1561−1569.
(29) Soni, S. S.; Brotons, G.; Bellour, M.; Narayanan, T.; Gibaud, A. *J. Phys. Chem. B* **2006**, *110*, 15157−15165.
(30) Ivanova, R.; Lindman, B.; Alexandridis, P. *Langmuir* **2000**, *16*, 3660−3675.
(31) Wadsten-Hindrichsen, P.; Bender, J.; Unga, J.; Engstrom, S. *Colloid Interface Sci.* **2007**, 315, 701−713.
(32) Libster, D.; Aserin, A.; Wachtel, E.; Shoham, G.; Garti, N. *J. Colloid Interface Sci.* **2007**, *308*, 514−524.
(33) Siddig, M. A.; Radiman, S.; Jan, L. S.; Muniandy, S. V. *Colloids Surf., A* **2006**, *276*, 15−21.
(34) Lake, J. A. *Acta Crystallogr.* **1967**, *23*, 191−194.
(35) Landh, T. *J. Phys. Chem.* **1994**, *98*, 8453−8467.
(36) Popescu, G.; Barauskas, J.; Nylander, T.; Tiberg, F. *Langmuir* **2007**, *23*, 496−503.
(37) Lindblom, G.; Larsson, K.; Johansson, L.; Fontell, K.; Forsén, S. *J. Am. Chem. Soc.* **1979**, *101*, 5465−5470.
(38) Borné, J.; Nylander, T.; Khan, A. *Langmuir* **2000**, *16*, 10044−10054.
(39) Glasel, J. A. In *Water a Comprehensive Treatise*; Franks, F., Ed.; Plenum Press: New York, 1972; Vol. 1, p 215.
(40) Jones, J. L.; McLeish, T. C. B. *Langmuir* **1999**, *15*, 7495−7503.
(41) Mezzenga, R.; Meyer, C.; Servais, C.; Romoscanu, A. I.; Sagalowicz, L.; Hayward, R. C. *Langmuir* **2005**, *21*, 3322−3333.
(42) Sagalowicz, L.; Mezzenga, R.; Leser, M. E. *Curr. Opin. Colloid Interface Sci.* **2006**, *11*, 224−229.
(43) Wang, H. X.; Zhang, G. Y.; Feng, S. H.; Xie, X. L. *Colloids Surf., A* **2005**, *256*, 35−42.
(44) Spicer, P. T.; Hayden, K. L.; Lynch, M. L.; Ofori-Boateng, A.; Burns, J. L. *Langmuir* **2001**, *17*, 5748−5756.
(45) Amar-Yuli, I.; Garti, N. *Colloids Surf., B* **2005**, *43*, 72−82.
(46) Hyde, S. T. In *Handbook of Applied Surface and Colloid Chemistry*, 1st ed.; Holmberg, K., Ed.; Wiley: New York, 2001; Chapter 16.
(47) Nilsson, P. G.; Lindman, B. *J. Phys. Chem.* **1983**, *87*, 4756−4761.
(48) Mezzenga, R.; Grigorov, M.; Zhang, Z. D.; Servais, C.; Sagalowicz, L.; Romoscanu, A. I.; Khanna, V.; Meyer, C. *Langmuir* **2005**, *21*, 6165−6169.
(49) Yethiraj, A.; Capitani, D.; Burlinson, N. E.; Burnell, E. *Langmuir* **2005**, *21*, 3311−3321.
(50) Feiweier, T.; Heil, B.; Pospiech, E. V.; Fujara, F.; Winter, R. *Phys. Rev. E* **2000**, *62*, 8182−8194.
(51) Liu, L.; John, V. T.; McPherson, G.; Maskos, K.; Bose, A. *Langmuir* **2005**, *21*, 3795−3801.
(52) Razumas, V.; Larsson, K.; Miezis, Y.; Nylander, T. *J. Phys. Chem.* **1996**, *100*, 11766−11774.
(53) Nilsson, A.; Holmgren, A.; Lindblom, G. *Biochemistry* **1991**, *30*, 2126−2133.
(54) Inoue, T.; Matsuda, M.; Nibu, Y.; Misono, Y.; Suzuki, M. *Langmuir* **2001**, *17*, 1833−1840.
(55) Hübner, W.; Mantsch, H. H. *Biophys. J.* **1991**, *59*, 1261−1272.
(56) Nilsson, A.; Holmgren, A.; Lindblom, G. *Chem. Phys. Lipids* **1994**, *71*, 119−131.